PHYSICAL REVIEW B VOLUME 16, NUMBER 5 1 SEPTEMBER 1977

Magnetic excitations in $NdAl_2$

A. Furrer

Institute for Reactor Technique, Swiss Federal Institute of Technology
CH-5303 Würenlingen, Switzerland

H.-G. Purwins

Solid State Physics Laboratory, Swiss Federal Institute of Technology,
CH-8093 Zürich, Switzerland

(Received 7 March 1977)

The magnetic excitation spectrum of the ferromagnet $NdAl_2$ has been studied at 4.2 K by neutron inelastic scattering. Three acoustical, three optical branches, and partly a fourth optical branch have been resolved. Crystal-field and exchange parameters have been obtained by analyzing the results in terms of a pseudoboson theory that includes all ten levels of the free-ion ground state of Nd^{3+}. A good description of the observed excitation energies and intensities is obtained. The reliability of the model parameters is supported by internal consistency checks and by comparison with various physical properties of $NdAl_2$. The interatomic exchange parameters exhibit a Ruderman-Kittel-Kasuya-Yosida-like qualitative behavior.

I. INTRODUCTION

Considerable improvement has been obtained in recent years in understanding the magnetism of rare-earth (R) metals and intermetallic compounds where crystal-field effects are important.[1-3] The basic idea is that only $4f$ electrons of the RE ion contribute a magnetic moment and that these f electrons are well localized. Insofar as magnetic properties are concerned the interaction of the $4f$ electrons with the surrounding of the RE ion can be represented by an electrostatic potential (crystal field) which produces a Stark splitting of the free-ion multiplets. For the high point symmetry of the RE site only a small number of parameters is necessary to describe the splitting.[4] In the case of magnetic interactions one has to add to the crystal field an exchange term which is usually assumed to be of Heisenberg type. In the single-ion approximation the exchange interaction is treated by an effective field which produces a splitting of the crystal-field split $4f$ levels. Any transition in the single-ion scheme corresponds to a spin-wave-like elementary excitation when including the total exchange interaction. (For brevity we refer to this type of excitations as spin waves or magnons throughout the article.) A pseudoboson theory[5] has been developed by various authors to calculate the strength and the dispersion of these excitations from the poles of the dynamic magnetic susceptibility $\chi(\vec{q}, \omega)$.[6-8]

The interpretation of several neutron inelastic-scattering experiments shows that the pseudoboson theory is very useful to obtain an overall understanding of spin waves in RE intermetallic compounds.[9-18] For pure RE metals the situation is not quite clear since in principle a large number of crystal-field parameters has to be taken into account and there is no good argument to put one of these parameters to zero.[19] The situation is also complicated in the case where local and band magnetism appear at the same time as it is observed, e.g., in $Ho_{0.88}Tb_{0.12}Fe_2$.[20]

Although the experimentally determined magnon dispersion curves in RE metallic solids could be understood in several cases in terms of the pseudoboson theory there is almost no case where the used parameters are sufficiently reliable to obtain an unambiguous interpretation and a check of the internal consistency of the applied model. It is therefore interesting to measure the spin waves in a relatively simple system in which several dispersion branches can be observed and described by a small number of fit parameters. In the present paper we show that $NdAl_2$ is to a good extent such a material.

$NdAl_2$ has the $MgCu_2$ Laves phase structure in which the Nd^{3+} ions have a cubic point symmetry.[21] Since the Al ions are assumed to carry no magnetic moment the magnetic lattice is of the diamond type. Magnetic properties of $NdAl_2$ have been investigated intensively. The first magnetization measurements in-

dicated that $NdAl_2$ is ferromagnetic,[22] in agreement with susceptibility and neutron-diffraction experiments.[23] The most reliable value for the Curie temperature is obtained from specific-heat[24] and single-crystal elastic constants[25] both giving $T_C = 77.2$ K. Detailed magnetization measurements on single crystals in high fields reveal ⟨100⟩ as the easy direction of magnetization,[26,27] in agreement with Knight-shift results.[28] NMR measurements are interpreted in terms of a negative conduction-electron polarization at the Al sites.[29] (For a detailed discussion of NMR results see Sec. IV.) Preliminary neutron-inelastic-scattering experiments on single crystals of $NdAl_2$ measuring the magnon dispersion in the ⟨110⟩ (Ref. 12) and ⟨001⟩ (Ref. 17) direction of reciprocal space have been reported recently. The results of Ref. 17 show that at least three acoustical and three optical dispersion branches can be resolved.

In the present work we undertake a detailed and rather complete study of the spin waves in $NdAl_2$ at 4.2 K. In Sec. II we give a short description of the experimental procedure and we present the results. In Sec. III the experimental results are interpreted in terms of the pseudoboson theory using an isotropic Heisenberg exchange interaction and a cubic crystal field. In Sec. IV we discuss the results and we evaluate the interatomic exchange parameters. We also compare our results with earlier studies of $NdAl_2$ and other RAl_2 compounds. In Sec. V we draw some conclusions that may be allowed on the basis of the results of this work.

II. EXPERIMENTAL

The $NdAl_2$ compound was prepared from 99.9% Nd and 99.999% Al in a water-cooled silver crucible by melting the stoichiometric composition using the induction method. Single crystalline cylinders with the axes parallel to ⟨110⟩ were obtained by the Czochralski method from a tungsten crucible heated in a radio-frequency field. Typical impurity concentrations were of order of 0.1 at.% and the density of the crystals was 98.6% of the theoretical density. The mosaic spread of the crystals was about 20′.

The experiments were carried out using a triple-axis spectrometer at the reactor Diorit, Würenlingen. The constant-momentum-transfer (constant $\vec{Q}$) mode of operation was used throughout with variable incident-neutron energy. The scattered neutron energy was kept fixed at 5 meV (cooled beryllium filter in front of the analyzer) for excitation energies ≤ 2 meV and at 15 meV (pyrolytic-graphite filter in front of the analyzer) for excitation energies >2 meV. The (002) planes of pyrolytic-graphite crystals were used as monochromator and analyzer. The specimen consisted of four cylindrical single crystals of $NdAl_2$ aligned so as to have identical crystallographic orientations with a $[1\bar{1}0]$ axis normal to the scattering plane. The volumes of the single crystals ranged from 0.4 to 0.7 cm^3, and the total sample volume amounted to 2.1 cm^3. The resulting mosaic spread of the sample was about 30′. The measurements were done at 4.2 K.

The majority of the measurements were made with magnon wave vectors along the three principal symmetry directions around the (111), (002), and (220) reciprocal-lattice points. In $NdAl_2$ there are two neodymium ions per unit cell, so that the spin-wave spectrum is separated into optical and acoustical branches. We are able to distinguish between optical and acoustical modes through the magnon structure factor (see Sec. III). We can observe in the (220) Brillouin zone only the acoustical spin-wave branches and in the (002) zone only the optical spin-wave branches, while in the (111) zone both the acoustical and the optical structure factors are nonzero. Figure 1 shows energy spectra of neutrons scattered from $NdAl_2$ observed at the center of the acoustic zone (220), the zone boundary (003), and the center of the optical zone (002). The magnetic origin of the observed peaks has been confirmed by measurements at different momentum transfers, and the mode assignments were made by comparing the observed spin-wave energies and peak intensities with the values calculated from the model

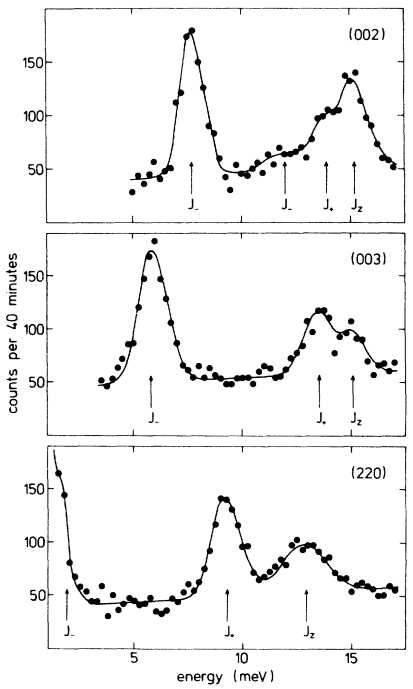

FIG. 1. Energy spectra of neutrons scattered from $NdAl_2$ at 4.2 K observed in measurements at the centers of the optical (002) and acoustical (220) zones and at the zone boundary (003). The lines denote Gaussian functions adapted to the experimental profiles by the least-squares method. The branch labels are assigned on the basis of the model calculations.

(see Sec. III). Direct phonon scattering did not disturb the observed energy spectra, since the phonon peaks were less intense than the magnon lines by an order of magnitude at least. At (002) four optical spin-wave modes are observed, while the energy spectrum taken at (003) exhibits only three spin-wave modes. Three acoustic spin-wave modes appear in the energy spectrum taken at (220). Here, the J_- mode is strongly contaminated by the elastic line. In order to resolve the energy gap of the J_- branch completely, measurements have been performed with increased energy resolution. The result is shown in Fig. 2.

The spin-wave dispersions of $NdAl_2$ determined in the present experiments are shown in Figs. 3, 4, and 5. Three acoustical and three optical spin-wave branches are resolved. A fourth branch has only been observed close to the optical zone center, because its intensity is strongly decreasing by going to the optical zone boundary and to the acoustical zone. The acoustical and optical branches of each spin-wave mode are degenerate at the zone boundary for the ⟨001⟩ and ⟨110⟩ direction by symmetry.

III. ANALYSIS OF RESULTS

We describe the Hamiltonian of the spin system of $NdAl_2$ as the sum of crystalline electric-field and exchange interaction terms:

$$\mathcal{H} = \mathcal{H}_{cf} + \mathcal{H}_{ex} . \tag{1}$$

For the polar axis along the cube edge (easy direction of magnetization) the crystal-field term has the form

$$\mathcal{H}_{cf} = \sum_{i=k,m} B_4(\hat{O}_{4i}^0 + 5\hat{O}_{4i}^4) + B_6(\hat{O}_{6i}^0 - 21\hat{O}_{6i}^4) , \tag{2}$$

where B_u are crystal-field parameters and $\hat{O}_u^v$ are Stevens operator equivalents.[30] We assume that the exchange coupling between the total angular momentum operators $\hat{J}$ is of simple Heisenberg type:

$$\mathcal{H}_{ex} = -\sum_{k\neq l} \mathcal{J}(\vec{R}_k - \vec{R}_l)\hat{J}_k\cdot\hat{J}_l - \sum_{m\neq n} \mathcal{J}(\vec{R}_m - \vec{R}_n)\hat{J}_m\cdot\hat{J}_n - \sum_{k,m} \mathcal{J}(\vec{R}_k - \vec{R}_m)\hat{J}_k\cdot\hat{J}_m , \tag{3}$$

where the summation indices k,l and m,n refer, respectively, to the two interpenetrating face-centered-cubic sublattices of the diamond lattice built by the rare-earth ions. Equation (1) is solved by the pseudoboson method[5] in which the magnetic excitation spectrum is given by the poles of the dynamic magnetic susceptibility[6–8]:

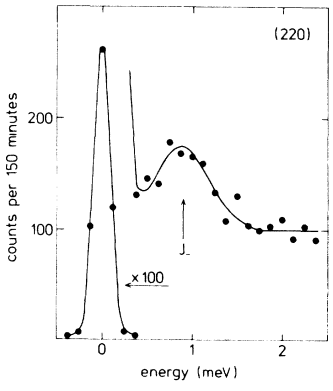

FIG. 2. High-resolution energy spectrum of neutrons scattered from $NdAl_2$ at 4.2 K observed in a measurement at the center of the acoustical (220) zone. The lines and the branch label are as in Fig. 1.

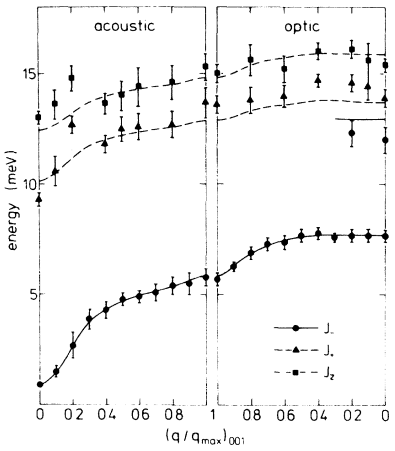

FIG. 3. Magnon dispersion curves of $NdAl_2$ at 4.2 K for wave vectors along ⟨001⟩. The lines represent the best fit to the pseudoboson model.

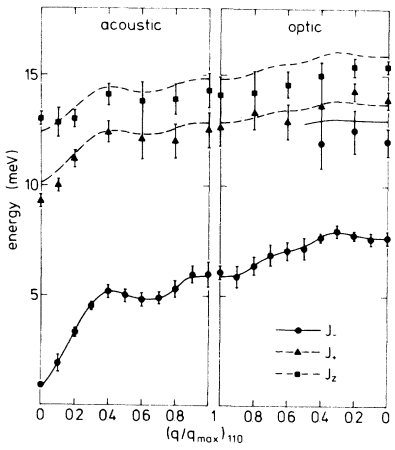

FIG. 4. Magnon dispersion curves of $NdAl_2$ at 4.2 K for wave vectors along ⟨110⟩. The lines are as in Fig. 3.

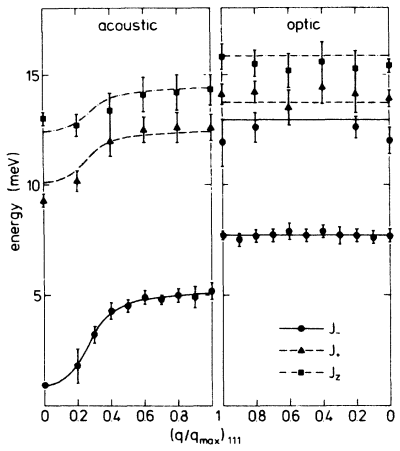

FIG. 5. Magnon dispersion curves of $NdAl_2$ at 4.2 K for wave vectors along $\langle 111\rangle$. The lines are as in Fig. 3.

$$\chi^{zz}(\vec{q},\omega)=\chi_0^{zz}(\omega)\times\{1-2[\mathcal{J}(\vec{q})\pm|\mathcal{J}'(\vec{q})|]\chi_0^{zz}(\omega)\}^{-1}\ , \tag{4a}$$

$$\chi^{+-}(\vec{q},\omega)=\chi_0^{+-}(\omega)\times\{1-[\mathcal{J}(\vec{q})\pm|\mathcal{J}'(\vec{q})|]\chi_0^{+-}(\omega)\}^{-1}\ , \tag{4b}$$

with

$$\chi_0^{\alpha\beta}(\omega)=\frac{(g\mu_B)^2}{Z(T)}\times\sum_{a\neq b}\frac{\langle a|\hat{J}_\alpha|b\rangle\langle b|\hat{J}_\beta|a\rangle}{E_a-E_b+\hbar\omega}\times\left[\exp\left(-\frac{E_a}{k_BT}\right)-\exp\left(-\frac{E_b}{k_BT}\right)\right]\ , \tag{5}$$

$$\mathcal{J}(\vec{q})=\sum_{k\neq l}\mathcal{J}(\vec{R}_k-\vec{R}_l)\times\exp[i\vec{q}\cdot(\vec{R}_k-\vec{R}_l)]\ , \tag{6a}$$

$$\mathcal{J}'(\vec{q})=\sum_{k,m}\mathcal{J}(\vec{R}_k-\vec{R}_m)\times\exp[i\vec{q}\cdot(\vec{R}_k-\vec{R}_m)]\ . \tag{6b}$$

$|a\rangle$, $|b\rangle$ and E_a, E_b are the single-ion eigenfunctions and energy eigenvalues of Nd^{3+} in $NdAl_2$ which are obtained by diagonalizing Eq. (1) in the molecular field approximation:

$$\mathcal{H}_{mf}=\mathcal{H}_{cf}-g\mu_BH_{mf}\sum_i\hat{J}_{iz} \tag{7}$$

with the molecular field

$$H_{mf}=(2/g\mu_B)[\mathcal{J}(0)+\mathcal{J}'(0)]\langle\hat{J}_z\rangle\ . \tag{8}$$

For each transition $|a\rangle\rightarrow|b\rangle$ defined by the single-ion dynamic susceptibility [Eq. (5)] we obtain one acoustical and one optical dispersion branch corresponding to the upper and lower sign in Eq. (4), respectively. $\mathcal{J}(\vec{q})$ is real, while $\mathcal{J}'(\vec{q})$ is complex because the vector joining sites on different sublattices is not a lattice vector. For the particular case of wave vectors $\vec{q}$ along $\langle 110\rangle$ and $\langle 001\rangle$ $\mathcal{J}'(\vec{q})$ is real.

In the analysis of the observed spin-wave spectra one has to perform an intensity calculation in order to identify uniquely the various transitions. The differential neutron cross section for spin-wave scattering is given by[31]

$$\frac{d^2\sigma}{d\Omega\,d\omega}\sim\frac{k_1}{k_0}F^2(\vec{Q})[1\pm\cos(\vec{\tau}\cdot\vec{\rho}+\phi)]\times\mathrm{Im}\{\chi^{zz}(\vec{q},\omega)+\tfrac{1}{2}[\chi^{+-}(\vec{q},\omega)+\chi^{-+}(\vec{q},\omega)]\}\times\{n(\omega)\delta(\epsilon_0-\epsilon_1+\hbar\omega)+[n(\omega)+1]\delta(\epsilon_0-\epsilon_1-\hbar\omega)\}\times\sum_{\vec{\tau}}\Delta(\vec{Q}-\vec{\tau}-\vec{q})\ , \tag{9}$$

where the upper and lower sign refers to the acoustical and optical spin-wave branches, respectively. k_0, k_1 and ϵ_0, ϵ_1 are the wave numbers and energies of the incoming and scattered neutrons, respectively, $F(Q)$ is the magnetic form factor, $n(\omega)$ the Bose occupation number, $\vec{\rho}$ the vector joining a Nd ion in one sublattice to its nearest neighbor in the other sublattice, and ϕ denotes the phase angle determined by

$$\mathcal{J}'(\vec{q})=|\mathcal{J}'(\vec{q})|\exp(i\phi)\ . \tag{10}$$

In general ϕ is not zero nor a multiple of π, except for $\vec{q}$ in the $\langle 110\rangle$ and $\langle 001\rangle$ direction.

A least-squares fitting procedure based on the Hamiltonian (1) as described in the preceding paragraphs has been applied to the observed spin-wave energies of $NdAl_2$. The fitting parameters were B_4, B_6, $\mathcal{J}(\vec{q})$ and $|\mathcal{J}'(\vec{q})|$. In a first step the fit was carried out for each wave vector $\vec{q}=\frac{1}{5}n\vec{q}_{max}$ $(n=0,1,\ldots,5)$ separately, where $\vec{q}_{max}$ is the wave vector at the zone boundary for the three symmetry directions. Besides $\mathcal{J}(\vec{q})$ and $|\mathcal{J}'(\vec{q})|$ we obtained for each wave vector $\vec{q}$ a set of single-ion parameters B_4, B_6 and $\mathcal{J}(0)+\mathcal{J}'(0)$. The mean values of these parameters are

$$B_4=(-9.9\pm0.2)\times10^{-4}\ \text{meV}\ ,$$

$$B_6=(4.0\pm0.1)\times10^{-5}\ \text{meV}\ ,$$

$$\mathcal{J}(0)+\mathcal{J}'(0)=0.37\pm0.01\ \text{meV}\ .$$

In no case a deviation from these mean values of more than 6% was observed. The deviations are even

less than 4% if we exclude the results obtained for $\vec{q}_{001} = 0.2\vec{q}_{max}$. Then, keeping the single-ion parameters constant, $\mathcal{J}(\vec{q})$ and $|\mathcal{J}'(\vec{q})|$ have been determined for each wave vector $\vec{q} = \frac{1}{10} n \vec{q}_{max}$ $(n = 0, 1, \ldots, 10)$ from the energies of the lowest acoustical and optical spin-wave branches which are much better resolved than the higher spin-wave branches. The resulting exchange parameters $\mathcal{J}(\vec{q})$ and $|\mathcal{J}'(\vec{q})|$ are given in Fig. 6, and the spin-wave energies calculated from the model parameters are shown as lines in Figs. 3, 4, and 5. Observed and calculated energies are in good agreement.

In Fig. 7 we give the single-ion level scheme as a function of molecular field using the crystal-field parameters determined in the present experiments. From Eq. (4) we expect spin-wave energies close to the single-ion transition energies when $\mathcal{J}(\vec{q}) \pm |\mathcal{J}'(\vec{q})|$ is small. From Fig. 6 we see that this is the case near the zone boundary along $\langle 001 \rangle$ and $\langle 110 \rangle$. In fact the agreement of the magnon energies (Figs. 3 and 4) and the single-ion transition energies (Fig. 7) listed in Table I is good. In Table I we give also the matrix elements for dipole transitions between the ground state $|0\rangle$ and the excited states $|a\rangle$. Since the neutron cross section for spin-wave scattering is approximately proportional to $|\langle a|\hat{J}_\alpha|0\rangle|^2$, the strongest ground-state transitions are therefore the longitudinal transition to the fifth excited state and three transverse transitions to the first, third, and fourth excited states. Transitions to the exchange split $\Gamma_8^{(2)}$ quartet excited state are less intense and have not been observed in the present experiments.

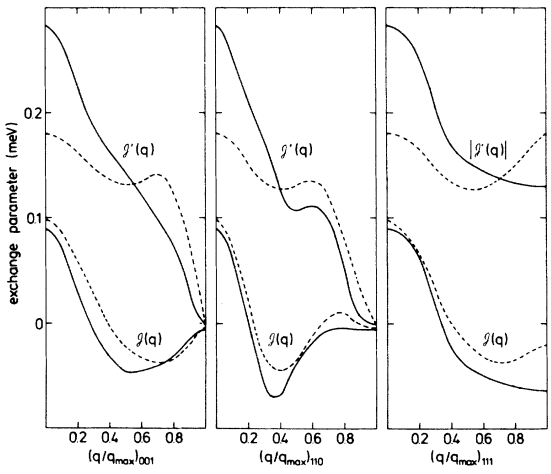

FIG. 6. Exchange parameters $\mathcal{J}(\vec{q})$ and $\mathcal{J}'(\vec{q})$ for $NdAl_2$ (full lines) at 4.2 K in the three symmetry directions. The dashed lines represent the results obtained for $TbAl_2$ (Ref. 10).

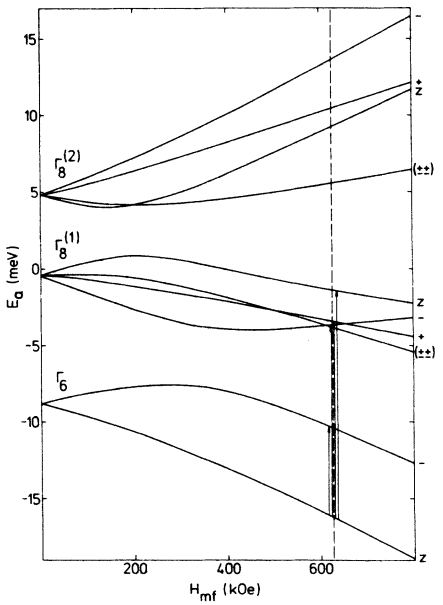

FIG. 7. Single-ion energy levels of Nd^{3+} in $NdAl_2$ at $T = 0$ as a function of the molecular field H_{mf}. The vertical dashed line corresponds to $\mathcal{J}(0) + \mathcal{J}'(0) = 0.37$ meV and the arrow heads indicate the four observed transitions. The level symmetry is given in the notation of Buyers *et al.* (Ref. 32).

IV. DISCUSSION

In the preceding section we applied a relatively simple theory to describe the dispersion of spin waves observed in $NdAl_2$ at low temperature. For a given wave vector $\vec{q}$ we use five parameters to fit six or seven spin-wave energies. In our model the single-ion parameters are independent of $\vec{q}$. The fact that the fitted parameters B_4, B_6 and $\mathcal{J}(0) + \mathcal{J}'(0)$ vary only by 6% (4% when we exclude the result at $\vec{q}_{001} = 0.2\vec{q}_{max}$)

TABLE I. Energy levels E_a and matrix elements of $\hat{J}_\alpha$ for Nd^{3+} in $NdAl_2$ corresponding to the single-ion parameters determined in the present experiments.

a	E_a (meV)	$\langle a\|\hat{J}_+\|0\rangle$	$\langle a\|\hat{J}_-\|0\rangle$	$\langle a\|\hat{J}_z\|0\rangle$	$\langle a\|\hat{J}_z\|a\rangle$
0	0	0	0	3.570	3.570
1	5.84	0	3.253	0	3.029
2	12.41	0	0	0	2.234
3	12.52	0	-1.260	0	-0.630
4	12.79	-2.280	0	0	1.384
5	14.78	0	0	1.707	1.270
6	21.71	0	0	0	-1.234
7	25.45	0	0	0.018	-3.340
8	26.60	0.568	0	0	-2.384
9	29.77	0	-0.702	0	-3.899

is a strong support for the internal consistency of our interpretation. The single-ion parameters are within experimental error in very good agreement with the results of earlier inelastic neutron measurements[12] which gave $B_4 = -1.0\times10^{-3}$ meV, $B_6 = 4.0\times10^{-5}$ meV and $\mathcal{J}(0) + \mathcal{J}'(0) = 0.372$ meV. From the single-ion parameters of $NdAl_2$ we calculate the molecular field Curie temperature to be $T_{C,mf} = 63 \pm 3$K which is considerably lower than the most reliable experimental value of $T_C = 77.2$ K. However, a discrepancy of this order of magnitude is expected due to the failure of molecular field theory near the phase transition.

With the knowledge of the single-ion parameters B_4, B_6 and $\mathcal{J}(0) + \mathcal{J}'(0)$ various magnetic properties can be calculated in the molecular field approximation. For a comparison of such calculations with experiment detailed data are available for the single-crystal bulk magnetization,[26,27] for the sound velocity,[25] for the magnetostriction,[27] for the low-temperature ground-state wave function obtained by means of polarized neutron diffraction,[33] for the specific heat[24] and for the susceptibility.[23] The latter, however, does not provide a sensitive test of our model and will not be further discussed, since crystal-field effects do not significantly influence the paramagnetic susceptibility of $NdAl_2$.

The single-ion parameters of $NdAl_2$ have been used to calculate the magnetization as a function of magnetic field applied in the $\langle 001\rangle$, $\langle 110\rangle$, and $\langle 111\rangle$ directions using a two-dimensional mean-field theory.[26,34] The calculated values are in good agreement with the experimental data.[26] Similar results have been obtained in a less rigorous analysis of the single-crystal magnetization of $NdAl_2$ including a discussion of magnetostrictive effects.[27] On the basis of a point-charge model the authors calculated a second-order crystal-field parameter $B_2 = -2.4\times10^{-3}$ meV due to a tetragonal magnetostrictive distortion of $\delta = 10^{-3}$. Although it is merely a matter of luck whether one can obtain good crystal-field parameters from a point-charge calculation it is interesting enough that the analysis of elastic constants of $NdAl_2$ in terms of magnetoelastic coupling parameters[25] leads to a value of $|B_2| = 2.8\times10^{-3}$ meV for $\delta = 10^{-3}$. On the basis of these findings one might be inclined to take a second-order crystal-field term into account in Eq. (2) to improve the agreement between calculated and observed spin-wave energies. However, test calculations show that a value of B_2 at least an order of magnitude larger than the above mentioned number is necessary to obtain some improvement. The same is true also for the bulk magnetization calculations. Therefore it seems to us more likely that other effects are the predominant sources for the small residual discrepancies in the magnon dispersion curves and in the magnetization.

From elastic scattering of polarized neutrons magnetization density maps have been obtained for $NdAl_2$.[33] From these data the low-temperature single-ion ground-state wave function of Nd^{3+} in $NdAl_2$ could be determined to be $\psi = 0.885|\frac{9}{2}\rangle + 0.451|\frac{1}{2}\rangle - 0.112|-\frac{7}{2}\rangle$ which is in reasonable agreement with $\psi = 0.877|\frac{9}{2}\rangle + 0.478|\frac{1}{2}\rangle + 0.043|-\frac{7}{2}\rangle$ obtained from the present work.

The single-ion parameters of $NdAl_2$ have been used to calculate the magnetic specific heat.[34] The agreement with experiment[24] is satisfactory although the calculated values are shifted towards lower temperature because of the discrepancy between the molecular-field Curie temperature and the experimental T_C.

Qualitative information on the crystal-field parameters of $NdAl_2$ has been obtained from NMR measurements. From the easy direction of magnetization of $NdAl_2$ the signs of B_4 and B_6 could be predicted[28] in agreement with the present work.

Beside the single-ion properties which are a probe for the electrostatic field and the mean exchange field we obtain from our experiments detailed information about the exchange forces via the dispersion of the spin waves. Since our experiments yield results in reciprocal space, it is illuminating to transform $\mathcal{J}(\vec{q})$ and $\mathcal{J}'(\vec{q})$ of Eq. (6) into real space and to evaluate interatomic exchange parameters. In the calculation we adjust first the exchange parameter between the nearest neighbors. We then include successively higher-order neighbors each time varying also the $n-1$ foregoing parameters when including the n th parameter. By this procedure we obtain ten interatomic exchange parameters as given in Fig. 8.

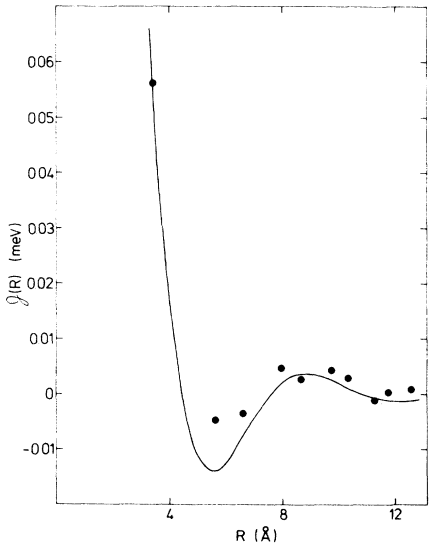

FIG. 8. Interatomic exchange parameters $\mathcal{J}(R)$ of $NdAl_2$ at 4.2 K as a function of distance R. The line represents the best fit of the RKKY theory to $\mathcal{J}(R)$.

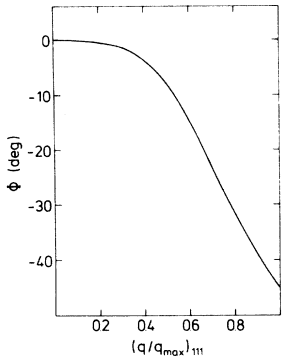

FIG. 9. The phase angle ϕ of Eq. (10) for wave vectors along ⟨111⟩.

With the help of the interatomic exchange parameters $\mathcal{J}(\vec{R})$ and Eq. (6b) we calculate the real and imaginary part of $\mathcal{J}'(\vec{q})$ along ⟨111⟩ of which only the absolute can be directly obtained from experiment. The resulting phase angles ϕ [defined by Eq.(10)] are shown in Fig. 9.

In order to check the wave functions obtained from the applied pseudoboson theory we compare the intensities calculated from the cross-section formula (9) with the intensities of the observed neutron groups. All the factors resulting from instrumental and resolution effects are taken into account. The results are shown in Figs. 10, 11, and 12, where the intensity scale corresponds to the residues of

$$\mathrm{Im}\{\chi^{zz}(\vec{q},\omega)+\tfrac{1}{2}[\chi^{+-}(\vec{q},\omega)+\chi^{-+}(\vec{q},\omega)]\}\,.$$

The calculated values and particularly the intensities for the ⟨111⟩ direction using the phase angles ϕ given in Fig. 9 are in reasonable agreement with experiment. This serves as another strong support of the consistency of our model.

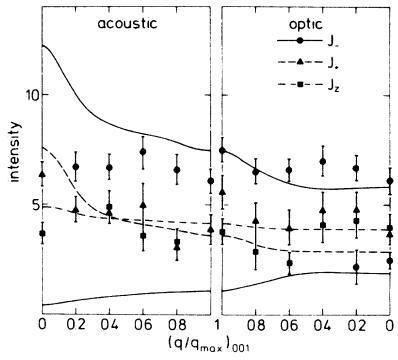

FIG. 10. Intensities of neutron groups due to spin-wave scattering in $NdAl_2$ at 4.2 K along ⟨001⟩. The lines represent the values calculated from the cross-section formula. The results for the intense J_- mode at the optical zone boundary are used to normalize the intensities.

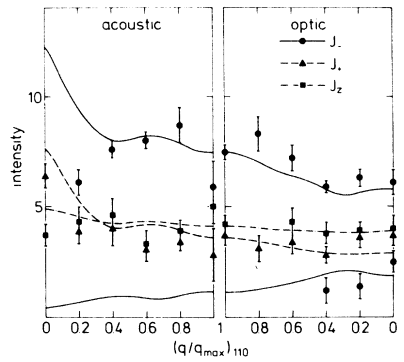

FIG. 11. Intensities of neutron groups due to spin-wave scattering in $NdAl_2$ at 4.2 K along ⟨110⟩. The lines and the intensity normalization are as in Fig. 10.

It is interesting to compare the interatomic exchange parameters (Fig. 9) with the predictions of the Ruderman-Kittel-Kasuya-Yosida (RKKY) mechanism describing the interaction in terms of an exchange polarized free electron gas.[35] We do not expect to understand the exchange mechanism in terms of this theory in detail because a complicated compound like $NdAl_2$ is not likely to have a sea of free conduction electrons. However, since the RKKY mechanism is currently used in the interpretation of various magnetic properties it is worthwhile to discuss this point in detail for the case of $NdAl_2$ since the present work provides so detailed information.

For angular momentum $\hat{J}$ in a free electron gas of density N/V, Fermi wave vector $\vec{k}_F$, Fermi energy ϵ_F, and interaction parameter j between localized spins and conduction-electron spins we obtain[35]

$$\mathcal{J}(R) = Af(2k_FR)$$
$$= A\frac{\sin(2k_FR)-2k_FR\cos(2k_FR)}{(2k_FR)^4} \qquad (11a)$$

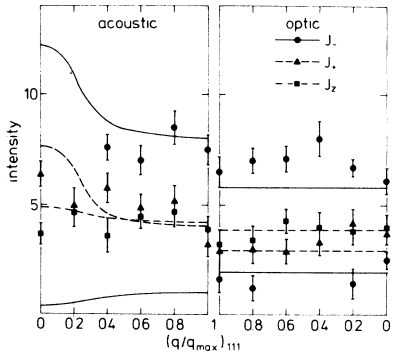

FIG. 12. Intensities of neutron groups due to spin-wave scattering in $NdAl_2$ at 4.2 K along ⟨111⟩. The lines and the intensity normalization are as in Fig. 10.

with

$$A = \frac{3(g-1)^2 j^2 (N/V)^{-1} k_F^3}{8\pi\epsilon_F} . \quad (11b)$$

The main qualitative features of $\mathcal{J}(R)$ are the strong decrease with increasing interatomic distance R and the oscillatory behavior. The best fit of Eq. (11) to $\mathcal{J}(R)$ (assumed to be isotropic) is obtained for $k_F = 0.50$ Å^{-1} and $A = 2.78$ meV and is drawn as a continuous line in Fig. 8. We see that the RKKY function gives a qualitative description of the interatomic exchange parameters evaluated from the spin-wave data. However, the quantitative agreement is not good, and a Fermi wave vector of $k_F = 0.50$ Å^{-1} is very small for an ordinary metal if a free electron gas is assumed. Indeed, if we believe that the Nd and Al atoms in $NdAl_2$ contribute each three electrons to the conduction band we obtain $k_F = 1.60$ Å^{-1}.

In this context a comparison with NMR work on $NdAl_2$ is of interest in which a negative conduction-electron polarization is reported.[29] This result can be related to the Fermi wave vector k_F since in the RKKY theory the conduction-electron polarization is proportional to $\sum_k f(2k_F R_k)$, where R_k is the distance between a given Al site and the kth RE ion. From NMR measurements on $NdAl_2$ values for the Fermi wave vector of $k_F = 2.10$ Å^{-1},[28] and $k_F = 1.5$ Å^{-1},[36] were derived. Beside the discrepancy in Fermi wave vector k_F we obtain from the present work a positive conduction-electron polarization when evaluating the appropriate sum. Apparently a consistent quantitative interpretation is not possible within the framework of the RKKY theory.

Finally a comparison of the results of $NdAl_2$ shall be given with measurements on other isostructural ferromagnetic RAl_2 compounds where a reliable evaluation of data exists. For the crystal-field parameters B_4 and B_6 this is done in Table II. We give also the reduced crystal-field parameters

$$A_n a^{n+1} = B_n a^{n+1} / \langle r^n \rangle \chi_n , \quad (12)$$

where a is the lattice constant, $\langle r^n \rangle$ the relativistic free-ion radial integral[37] and χ_n the reduced free-ion matrix element.[30] We note that the reduced crystal-field parameters $A_4 a^5$ and $A_6 a^7$ for different $R Al_2$ compounds vary by only 20% and 30%, respectively, which could be the uncertainty of the radial integrals $\langle r^n \rangle$ used in the calculation. The value of $A_6 a^7$ for $TbAl_2$ is rather small. However, the magnetization is not very sensitive to B_6 so that B_6 contains a large error when deduced from experiment.

In the simplest model the exchange parameters scale with the de Gennes factor $(g-1)^2$. However, this is only a very rough rule, and by comparing the Curie temperatures T_C of all $R Al_2$ compounds it can be shown that the rule is wrong by a factor of 4. Nevertheless it is interesting to compare the $\mathcal{J}(\vec{q})$ and $\mathcal{J}'(\vec{q})$ of $NdAl_2$ and $TbAl_2$ for which reliable exchange parameters exist. This is done in Fig. 6. The amazing feature of the functional behavior of $\mathcal{J}(\vec{q})$ of $TbAl_2$ is its similarity to the corresponding curves of $NdAl_2$.

V. CONCLUSIONS

We investigated a magnetically ordered RE system where the number of parameters necessary for the interpretation of the spin-wave spectra is sufficiently low and the experimental results sufficiently detailed to allow for a rigorous test of the pseudoboson theory. In fact we could carry out a straightforward interpretation supported by various internal consistency checks and by detailed comparisons with independent measurements. We therefore conclude that the pseudoboson theory in its simplest form (cubic crystal field and isotropic Heisenberg exchange) is the appropriate approach to understand the spin waves in $NdAl_2$ at low temperature.

Beside accurate crystal-field parameters we give also the detailed behavior of the exchange parameters in reciprocal and in real space. A quantitative interpretation of these data in terms of an RKKY interaction mechanism leads to unsurmountable difficulties. We

TABLE II. Crystal-field parameters of ferromagnetic RAl_2 compounds.

Compound	B_4 (10^{-4} meV)	B_6 (10^{-6} meV)	$A_4 a^5$ (10^4 meV Å)	$A_6 a^7$ (10^6 meV Å)	Ref.
$PrAl_2$	-44	-88	55	-4.3	38
	-38	-54	48	-2.7	16
$NdAl_2$	-10	40	37	-3.9	12
	-10.6	55	39	-5.3	27
	-9.9	40	36	-3.9	present work
$TbAl_2$	3.0	0.25	43	-1.6	38
$HoAl_2$	-0.69	0.64	42	-4.4	39
$ErAl_2$	1.10	-1.3	54	-6.3	40

therefore conclude that in $NdAl_2$ (and probably in all other ordered magnetic materials) a quantitative understanding of the exchange interaction cannot be obtained in terms of the simple RKKY theory. This means also that results obtained from NMR measurements using this theory cannot give reliable results. Nevertheless, our experiments show that the functional behavior of the exchange parameters is qualitatively consistent with the RKKY theory. However, the physical meaning of the leading parameters in particular the Fermi wave-vector should not be taken too literaly.

A comparison of the reduced crystal-field parameters of $NdAl_2$ with isostructural ferromagnetic RAl_2 compounds shows that they are very much the same for all compounds where a detailed evaluation of parameters is available. Comparing the behavior of the exchange parameters of $NdAl_2$ and $TbAl_2$ we see from Fig. 6 that the exchange functions $\mathcal{J}(\vec{q})$ are very similar, whereas $\mathcal{J}'(\vec{q})$ are different.

ACKNOWLEDGMENTS

We are grateful to Professor G. Busch and Professor W. Hälg for their support and for their interest in this work. We thank Professor M. Peter for allowing to use crystals prepared by one of the authors (H.-G.P.) at the Département de Physique de la Matière Condensée, Geneva. The permission to use the reactor Diorit at the EIR Würenlingen and the facilities of the Computation Center at the ETH Zürich as well as the expert technical assistance of A. Erdin, M. Koch, and R. Thut is gratefully acknowledged.

[1]R. J. Elliott, *Magnetic Properties of Rare Earth Metals* (Plenum, London, 1972).
[2]K. N. R. Taylor and M. I. Darby, *Physics of Rare Earth Solids* (Chapman and Hale, London, 1972).
[3]E. W. Wallace, *Rare Earth Intermetallics* (Academic, New York, 1973).
[4]See, for example, R. Lacroix, in *Théorie des groupes en physique classique et quantique,* edited by T. Kahan (Dunod, Paris, 1972), Vol. 3, p. 27.
[5]B. Grover, Phys. Rev. 140, A1944 (1965).
[6]W. J. L. Buyers, T. M. Holden, E. C. Svensson, R. A. Cowley, and M. T. Hutchins, J. Phys. C 4, 2139 (1971).
[7]I. Peschel, M. Klenin, and P. Fulde, J. Phys. C 5, L194 (1972).
[8]M. Klenin and I. Peschel, Phys. Kondens. Mater. 16, 219 (1973).
[9]T. M. Holden, E. C. Svensson, W. J. L. Buyers, and O. Vogt, in *Neutron Inelastic Scattering* (IAEA, Vienna, 1972), p. 553.
[10]W. Bührer, M. Godet, H.-G. Purwins, and E. Walker, Solid State Commun. 13, 881 (1973).
[11]H.-G. Purwins, J. G. Houmann, P. Bak, and E. Walker Phys. Rev. Lett. 31, 1585 (1973).
[12]J. G. Houmann, P. Bak, H.-G. Purwins, and E. Walker, J. Phys. C 7, 2691 (1974).
[13]T. M. Holden and W. J. L Buyers, Phys. Rev. B 9, 3797 (1974).
[14]T. M. Holden, E. C. Svensson, W. J. L. Buyers, and O. Vogt, Phys. Rev. B 10, 3864 (1974).
[15]A. Furrer, W. J. L. Buyers, R. M. Nicklow, and O. Vogt, Phys. Rev. B 14, 179 (1976).
[16]H.-G. Purwins, W. J. L. Buyers, T. M. Holden, and E. C. Svensson, AIP Conf. Proc. 29, 259 (1976).
[17]A. Furrer and H.-G. Purwins, Physica B 86-88, 189 (1977).
[18]B. Hennion, J. Pierre, D. Schmitt, and P. Morin, in *Crystal Field Effects in Metals and Alloys,* edited by A. Furrer (Plenum, New York, 1977), p. 19.
[19]A. R. Mackintosh and H. Bjerrum Møller, in *Magnetic Properties of Rare Earth Metals,* edited by R. J. Elliott (Plenum, London, 1972).
[20]R. M. Nicklow, N. C. Koon, C. M. Williams, and J. B. Milstein, Phys. Rev. Lett. 36, 532 (1976).
[21]J. H. Wernick and S. Geller, Trans. AIME 218, 866 (1960).
[22]H. J. Williams, J. H. Wernick, E. A. Nesbitt, and R. C. Sherwood, J. Phys. Soc. Jpn. 17, B1, 91 (1962).
[23]N. Nereson, C. Olsen, and G. Arnold, J. Appl. Phys. 37, 4575 (1966).
[24]C. Deenadas, A. W. Thompson, R. S. Craig, and W. E. Wallace, J. Phys. Chem. Solids 32, 1853 (1971).
[25]M. Godet and H.-G. Purwins, Helv. Phys. Acta 49, 821 (1976).
[26]G. J. Cock, L. W. Roeland, H.-G. Purwins, E. Walker, ar A. Furrer, Solid State Commun. 15, 845 (1974).
[27]B. Barbara, J. X. Boucherle, and M. F. Rossignol, Phys. Status Solidi A 25, 165 (1974).
[28]N. Kaplan, E. Dormann, K. H. J. Buschow, and D. Lebenbaum, Phys. Rev. B 7, 40 (1973).
[29]V. Jaccarino, B. T. Matthias, M. Peter, H. Suhl, and J. H. Wernick, Phys. Rev. Lett. 5, 251 (1960).
[30]K. W. H. Stevens, Proc. Phys. Soc. A 65, 209 (1952).
[31]W. Marshall and S. W. Lovesey, *Theory of Thermal Neutron Scattering* (Clarendon, Oxford, 1971).
[32]W. J. L. Buyers, T. M. Holden, and A. Perreault, Phys. Rev. B 11, 266 (1975).
[33]B. Barbara, J. X. Boucherle, J. P. Desclaux, M. F. Rossignol, and J. Schweizer, in *Crystal Field Effects in Metals and Alloys,* edited by A. Furrer (Plenum, New York, 1977), p. 168.
[34]P. Bak, J. Phys. C 7, 4097 (1974).
[35]T. Kasuya, Prog. Theor. Phys. 16, 45, 58 (1956); K. Yosida, Phys. Rev. 106, 893 (1957).
[36]E. Dormann, K. H. J. Buschow, K. N. R. Taylor, G. Brown, and M. A. A. Issa, J. Phys. F 3, 220 (1973).

[37] W. B. Lewis, *Proceedings of the XV Congress Ampere Bucharest,* edited by I. Ursu (Academy of Romania, Bucharest, 1970) p. 717.

[38] H.-G. Purwins, E. Walker, B. Barbara, M. F. Rossignol, and P. Bak, J. Phys. C 7, 3573 (1974).

[39] B. Barbara, J. X. Boucherle, and M. F. Rossignol, Phys. Lett. A 55, 321 (1975).

[40] H.-G. Purwins, E. Walker, B. Barbara, M. F. Rossignol, and A. Furrer, J. Phys. C 9, 1025 (1976).